PHYSICAL REVIEW B VOLUME 35, NUMBER 15 15 MAY 1987-II

Ion-beam-induced epitaxial vapor-phase growth: A molecular-dynamics study

Karl-Heinz Müller
Commonwealth Scientific and Industrial Research Organization, Division of Applied Physics, National Measurement Laboratory, Sydney, Australia 2070
(Received 5 May 1986; revised manuscript received 24 December 1986)

Low-energy ions which bombard a vapor-deposited film of low adatom mobility during growth mobilize surface atoms in the vicinity of the ion impact, causing a modification in the evolving microstructure. In a two-dimensional molecular-dynamics simulation where inert-gas ions strike a growing film of Lennard-Jones particles, it is demonstrated that ion bombardment during growth causes the filling of voids quenched in during vapor condensation and induces homoepitaxial growth. The dependence of film density and degree of homoepitaxial growth on the ion-to-vapor arrival rate ratio and ion energy is studied in detail.

I. INTRODUCTION

In recent years there has been an increasing interest in elucidating the mechanisms which lead to thin-film modifications caused by low-energy ion bombardment during growth,[1–3] as a detailed understanding is of importance for the preparation of new materials and novel devices that exhibit improved physical properties. Some ion-induced effects are acceleration of the nucleation stage,[4] enhanced adhesion,[5] modification of crystal structure[6] and film stress,[7] densification and, in the case of compound deposition, stoichiometric changes. Films grown under ion bombardment can be produced by a number of different techniques such as ion-assisted, sputter, or cluster-beam deposition. The evolving microstructure and properties of films depend strongly on the deposition technique since the impact energies and fluxes of ions and condensing film atoms are different for each method. For example, in ion-sputter deposition the sputtered atoms arrive at the substrate with a broad energy spectrum which ranges from about a tenth of an eV up to several eV.[8] Simultaneously, there will be bombardment from ions reflected from the target arriving at the film surface with energies of a few hundred eV depending on the primary ion energy and residual gas pressure. In magnetron sputtering[9] the growing film is bombarded by noble-gas ions created in a plasma formed near the substrate where the energy of the arriving ions can be influenced by an applied bias voltage. In ion-assisted vapor deposition,[10] modeled in this paper, the depositing material is evaporated by an electron gun and the bombarding ions emerge from a Kaufman source which produces monoenergetic ions of a well-defined flux which can be varied independently of the energy.

In order to predict desirable film modifications by ion bombardment, it is imperative to gain a detailed knowledge of the basic interaction mechanisms between ions and film species and their effects on film growth. Several attempts have been made to model ion-assisted thin-film growth by computer simulations. In Ref. 11 thermal spikes, created during film growth by impinging ions, were assumed to induce thermal hopping inside the expanding heat pulses. In Refs. 12 and 13, the binary-collision model was used to explain the densification of ion-assisted films in terms of ion incorporation and surface atom recoil implantation.

At present, the author is unaware of any publication on ion-assisted deposition described in terms of a molecular-dynamics (MD) simulation. Vapor deposition, in the absence of ion assistance, has been investigated by several authors using the MD model. Leamy *et al.*[14] compared MD results for vapor-deposited columnar film growth with the Henderson model[15] and emphasized the more realistic description of the MD simulations. Schneider *et al.*[16] performed a full three-dimensional MD computation which studied epitaxial growth from the vapor phase and the effect of substrate temperature.

The purpose of this paper is to investigate, by a two-dimensional MD simulation, ion-assisted vapor deposition of films of limited adatom mobility. As an example, Ar-ion-induced structural rearrangement processes which lead to the modification of a growing Ni film on a zero-temperature substrate will be examined at the atomic level. The dependence of the film packing density and the degree of homoepitaxial growth on deposition parameters like the ion-to-vapor flux ratio and the ion energy will be discussed.

II. MODEL

The effect of ions bombarding a piece of bulk material has been studied extensively by MD techniques, mainly to elucidate the atomic sputtering mechanism and invaluable conclusions, concerning its many-body nature, have been drawn.[17] These investigations were carried out for a model sample of ideal crystals with perfect surfaces and no crystal defects (where computer running time considerations limit the target to roughly 2000 atoms). Films grown from the vapor phase with limited adatom mobility like high-melting-point elements and some compound materials of high binding energy evolve on a room-temperature substrate in the form of porous columnar networks.[14,15,18–21] Such imperfect microstructures will be affected significantly by low-energy ion bombardment during growth because the ions induce additional adatom mobility. MD calculations are adequate to elucidate in

 ©1987 The American Physical Society

detail the effect of ion bombardment, because they are capable of describing the entire dynamics of all atoms involved and describe satisfactorily local freezing into new atomic configurations.

The simulation technique of MD is a classical model in which the evolution of a representative sample of a system is followed on the microscopic scale of time and distance. In our case the Hamilton's equations are solved for a system of interacting film atoms, arriving vapor atoms, and impinging ions. Ions are assumed to interact with the film atoms by a pairwise additive and spherically symmetric Molière potential[22] $V(r)$,

$$V(r)=\frac{Z_1Z_2e^2}{r}(0.35e^{-0.3r/a}+0.55e^{-1.2r/a}+0.1e^{-6.0r/a}) , \quad (1)$$

where a is the Firsov screening length[23]

$$a=0.4683(Z_1^{1/2}+Z_2^{1/2})^{-2/3} \quad (2)$$

and Z_1 and Z_2 are the atomic numbers of ion and film atom, respectively.

Two different atom-atom interactions between film atoms are used. One is a compound function, $U(r)$, which consists of a Molière repulsive "wall" ($Z_1=Z_2$) joined by a cubic spline[24] to a Lennard-Jones function, $U_{LJ}(r)$, attractive "well," where

$$U_{LJ}(r)=4\varepsilon\left[\left[\frac{\sigma}{r}\right]^{12}-\left[\frac{\sigma}{r}\right]^{6}\right] . \quad (3)$$

The other is a Lennard-Jones potential U_{LJ}. Figure 1 shows the atom-atom interactions U and U_{LJ}. The spline function joins the Molière potential at $r_a=1.6$ lattice units (1 l.u. $=1/2a_0$, $a_0\cong$ lattice distance) and the Lennard-Jones potential at $r_b=\sigma$. A value of 0.2239 nm for σ is determined such that it corresponds to the interatomic distance of fcc Ni in the (111) plane at equilibrium. The strength parameter, ε, in the Lennard-Jones potential, which determines the depth of the well, is selected to reproduce the cohesive energy of Ni with a two-dimensional close-packed lattice. The strength parameter ε is found to equal 1.32 eV. The potential U has a softer repulsive core than U_{LJ}. The reason for combining the Lennard-Jones and Molière potentials is that the repulsive Molière potential has been used successfully in many collision cascade calculations. As the calculations are two-dimensional and therefore reveal only qualitatively ion-assisted vapor-phase growth, no effort has been made to choose a more realistic potential. The interactions of Ni-Ni, Ar-Ni, and Ar-Ar are truncated at $r=2.5\sigma$, $37a_{\mathrm{Ni-Ni}}$ (screening length) and $37a_{\mathrm{Ar-Ni}}$, respectively. The attractive components of the Ar-Ni and Ar-Ar interactions are neglected since their wells are assumed to be very shallow.

In MD calculations of the equilibrium crystal vacuum interface, it is sufficient to use a simple forward difference scheme to integrate the equations of motion. In the case of nonequilibrium conditions where ions with large kinetic energies collide with film atoms, changes in force over a time step can be larger than in the equilibrium case. For our purposes, the average force method[25] which is based on a single iteration predictor-corrector operation

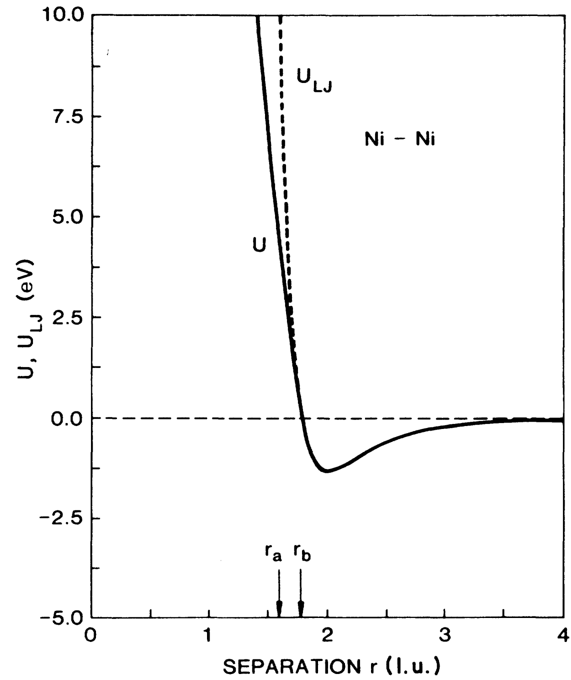

FIG. 1. Compound potential U representing the Ni-Ni interaction. The Molière potential defines U for $r<r_a$, the Lennard-Jones potential is valid for $r>r_b$. A cubic spline function determines U between r_a and r_b. The full Lennard-Jones potential is denoted by U_{LJ}.

seems suitable. Assuming particle i is at position $\mathbf{x}_i$ at time t and has a velocity $\mathbf{v}_i$, then the position and velocity at time $t+\Delta t$ is given by

$$\mathbf{x}_i(t+\Delta t)=\mathbf{x}_i(t)+\mathbf{v}_i(t)\Delta t+\langle \mathbf{F}_i\rangle\Delta t^2/2m_i , \quad (4)$$

$$\mathbf{v}_i(t+\Delta t)=\mathbf{v}_i(t)+\langle \mathbf{F}_i\rangle\Delta t/m_i , \quad (5)$$

where the average force on particle i is obtained as

$$\langle \mathbf{F}_i\rangle=\tfrac{1}{2}[\mathbf{F}_i(\mathbf{x}_i(t+\Delta t))+\mathbf{F}_i(\mathbf{x}_i(t))] \quad (6)$$

and

$$\mathbf{x}_i(t+\Delta t)=\mathbf{x}_i(t)+\mathbf{v}_i(t)\Delta t+\mathbf{F}_i(\mathbf{x}_i(t))(\Delta t)^2/2m_i . \quad (7)$$

The force exerted on particle i is determined by the surrounding configuration

$$\mathbf{F}_i=-\mathrm{grad}_i\sum_{j\ (j\neq i)}\phi(|\mathbf{x}_i-\mathbf{x}_j|) , \quad (8)$$

where ϕ is either U, U_{LJ}, or V depending on which species i and j represent.

The length of the integration time step, Δt, is readjusted for each calculation. In the case of $v_i>\langle F_i\rangle\Delta t/2m_i$, the maximum absolute velocity, $v_m=\max\{v_i\}$, is determined for each time and the new interval is calculated as $\Delta t=0.025a_0/v_m$. This method ensures that the maximum atomic displacement does not exceed 0.025 times the lattice distance during each calculation. When the involved particles slow down (or during film growth without ion bombardment), the integration time step, Δt,

is selected similar to other relaxation studies[16] as

$$\Delta t = 0.02(m\sigma^2/\varepsilon)^{1/2} , \quad (9)$$

where m is the mass of the Ni atom.

Because a vector computer CDC Cyber 205 is used for the computations, the MD code is designed to take advantage of its powerful vector processing facilities. For the generation of neighbor lists the "method of lights"[26] is employed with a fast vectorized sorting routine. Vectorization is further applied to the force computation which makes use of a force table look-up and interpolation procedure.

The two-dimensional rectangular simulation cell which contains the growing film is open along the positive z axis and the substrate consists of several close-packed rows of Ni-atoms which are placed parallel to the x axis above each other. The film atoms in the bottom layer are fixed at $z=0$ at their ideal lattice sites while atoms in the second layer are permitted to move. Whenever an atom moves downwards and crosses the second layer position at $z=(\sqrt{3}/2)a_0$, its velocity is reset to zero which means that the substrate behaves as an ideal heat sink of zero temperature. Periodic boundary conditions are applied in the x direction parallel to the substrate. Vapor atoms are introduced sequentially at random and impinge under a certain angle of incidence with respect to the film substrate normal. It is necessary to choose the elapsed time before introducing another vapor atom such that it is large enough to avoid interactions between incoming vapor atoms and also to give the system enough time so that impact-induced vibrations can relax and be absorbed in the lowest layer. (If the elapsed time chosen is too short, the vapor will condense on a film of elevated temperature thus the adatom mobility increases, resulting in a different structural evolution of the film.) Before introducing a new ion after every ν impinging vapor atoms (which correspond to an ion-to-vapor flux ratio of $j_I/j_V=\nu^{-1}$), the system is relaxed until all vapor atoms have arrived at the film surface to avoid possible collisions between a fast impinging ion and approaching vapor atoms. Before introducing more vapor atoms the system is allowed to relax after the ion-induced collision sequence. The elapsed time before a new vapor atom arrives is chosen to be at least 15 ps. The average temperature kT of the upper-film surface layers is calculated during deposition to ensure that vapor atoms condense at a cold surface ($kT<0.005\varepsilon$). Because of these cooling and relaxation requirements the calculations become very computer time consuming especially for larger j_I/j_V values. ($j_I/j_V=0.16$ with 780 particles involved, requires about 3 h CPU on a CDC Cyber 205 supercomputer.)

Before we discuss the results of our MD simulation for ion-assisted vapor deposition we have to mention the restrictions imposed by a two-dimensional (2D) model. The problem with a 2D calculation is that it restricts certain degrees of freedom of the interacting particles.[27] The removal of the kinetic energy from a 2D molecular-dynamics cell is slower than from a 3D one and some of the sputtering and atomic rearrangements occurring in the late stage of an ion impact may partially be thermal in origin. The great advantages of a 2D MD calculation are that it is computationally far less expensive and that it facilitates the tracking of particle trajectories, thus giving a simple pictorial description of ion-assisted thin-film deposition. Despite the above-mentioned disadvantages, a 2D MD simulation should reflect many of the essential features of a full 3D deposition.

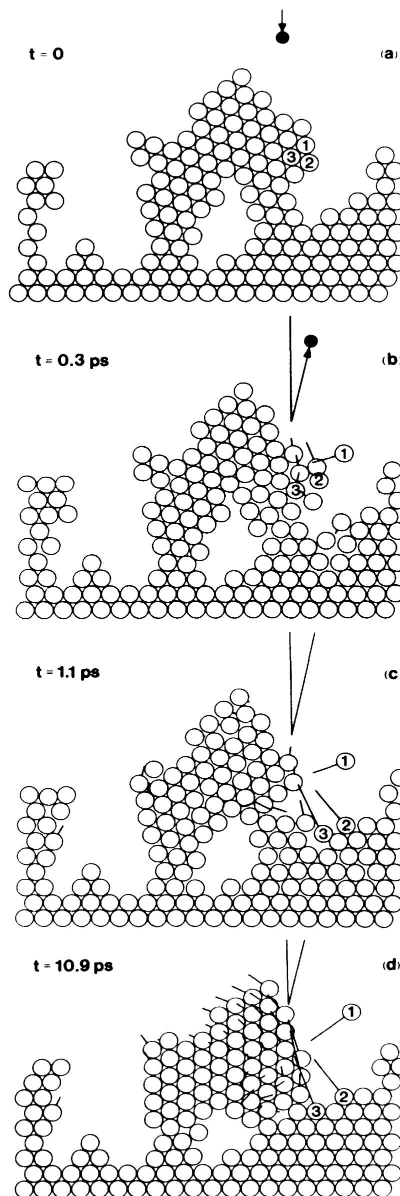

FIG. 2. (a) Film structure resulting from 120 condensing Ni vapor atoms approaching with an energy of 0.1 eV. The lowest two atomic layers represent the perfect Ni substrate. The vapor impingement angle is 30°. An Ar ion approaches the surface. (b)–(d) Collision sequence induced by a 100-eV Ar ion which hits the porous Ni film at $x=14a_0$.

III. RESULTS AND DISCUSSION

The structural rearrangements at an atomic level, caused by ions impinging on a growing film are complicated and therefore best represented pictorially. The film configuration is illustrated by depicting the positions of film atoms by open circles of radius $a_0/4$ and ions by solid circles. Instead of determining the kinetic energies of the vapor atoms from a Maxwellian distribution in a random fashion, a constant energy of 0.1 eV was assumed for simplicity. The vapor impact mobility at such a low kinetic energy is restricted to about one lattice distance and the vapor atom usually relaxes at its point of impact into the nearest cradle formed by two other film atoms[15,19–21]—a mechanism which is inherent in a MD calculation for a low-temperature substrate. Due to the low-vapor impact mobility, atomic shadowing occurs, causing the formation of voids and the growth of micro-columns.

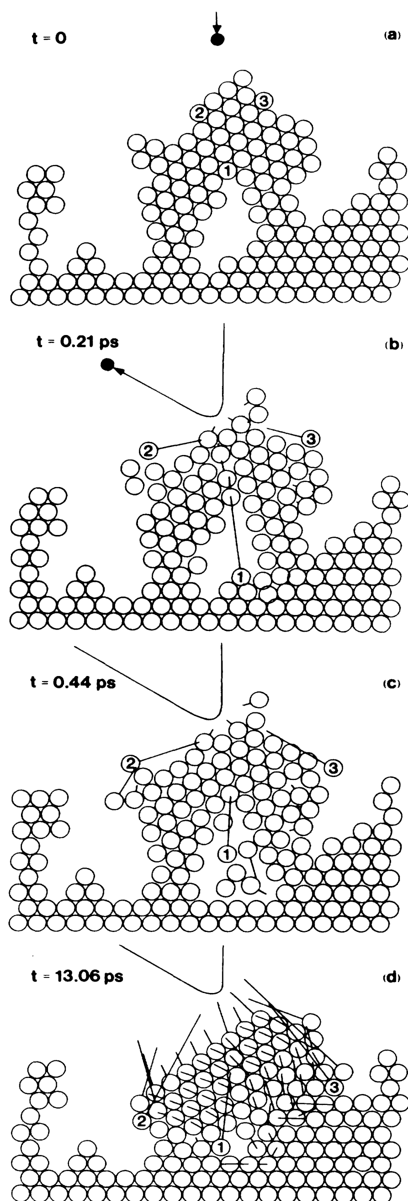

FIG. 3. (a)—(d) Collision sequence resulting from the impact of a 100-eV Ar ion hitting the porous Ni film at $x = 8.5a_0$.

Before discussing the structural modification obtained for different ion-to-vapor flux ratios and different ion energies,the typical effect of a single ion which hits the surface of a porous film is described. A typical structure formed by a few condensed vapor atoms is shown in Fig. 2(a), where the beginning of the formation of a porous columnar structure can be recognized. The vapor impingement angle relative to the substrate normal is 30°. Structure rearrangements occurring when an Ar ion of 100 eV strikes the surface at different points of the two-dimensional Ni film, is illustrated in Figs. 2 and 3. (Here the Ni-Ni interaction is of the compound form U.) A part of the kinetic energy of the ion is transferred to a few surface atoms which in turn transfer their kinetic energies to other film atoms so that a collision sequence evolves. The atomic displacements are indicated by straight lines (not trajectories) attached to the corresponding atoms with their origin at the atom's $t = 0$ positions. Displacements

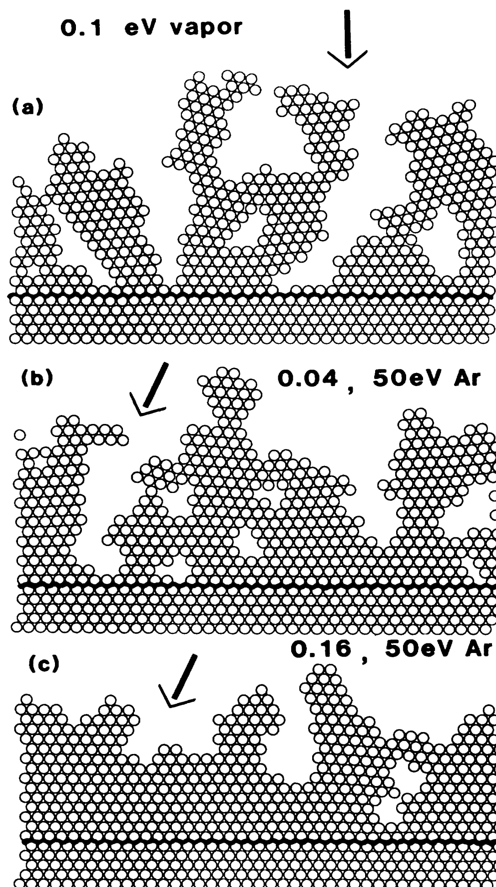

FIG. 4. (a)—(c) Typical microstructure obtained for condensing vapor atoms with kinetic energy of 0.1 eV arriving under normal incidence (a) without ion bombardment, (b) with Ar bombardment of $E = 50$ eV and $j_I/j_V = 0.04$, (c) with Ar bombardment of $E = 50$ eV and $j_I/j_V = 0.16$.

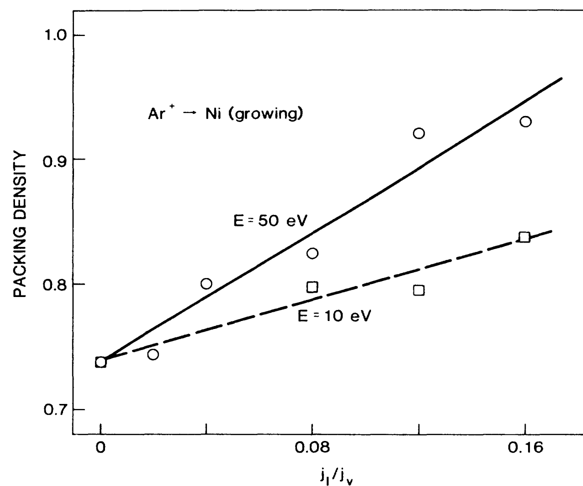

FIG. 5. Packing density (first nine layers above the substrate) vs ion-to-vapor flux ratio j_I/j_V for Ar ion kinetic energies $E=10$ and 50 eV. The atom-atom potential is $U_{\rm LJ}$.

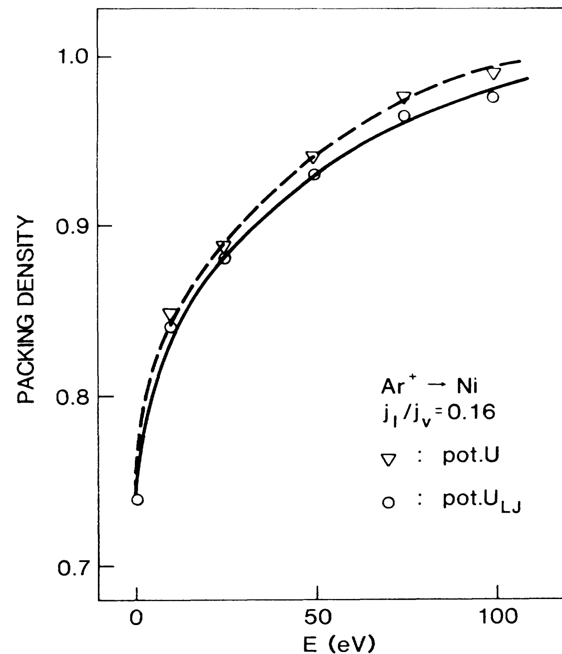

FIG. 7. Packing density (first nine layers above the substrate) vs Ar ion kinetic energy E for a fixed ion-to-vapor flux ratio $j_I/j_V=0.16$. Results for potentials U and $U_{\rm LJ}$ are shown.

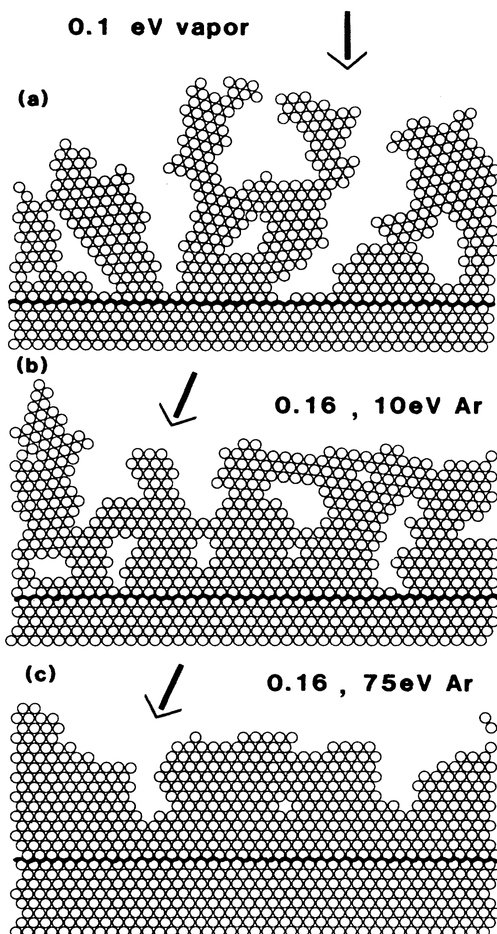

FIG. 6. (a)–(c) Typical microstructure obtained for condensing vapor atoms of 0.1 eV kinetic energy, arriving under normal incidence (a) without ion bombardment (b) with Ar bombardment of $E=10$ eV and $j_I/j_V=0.16$, (c) with Ar bombardment of $E=75$ eV and $j_I/j_V=0.16$. The atom-atom potential is U.

less than $a_0/2$ are not indicated. As can be seen from Fig. 2, ion bombardment during growth removes overhanging atoms and causes the void regions to remain open until filled by new depositing atoms. In addition, Fig. 3 shows that ions cause surface diffusion, local heating, and recrystallization. The initial violent ion-surface collision and the formation of knockon atoms require only about 0.2 ps while the freezing process, to establish the final atomic configuration, takes about 10 ps. As can be seen from Figs. 2 and 3 the structure rearranges such that atoms move to lower-lying positions where some undergo considerable displacements while a large number of atoms only become displaced slightly during the later stage of the relaxation process.

In the following the microstructure obtained when a large number of ions bombard the film during growth will be discussed. The vapor impingement angle is chosen to be 0° and the ion impingement angle 30°— a geometrical configuration which is frequently used in ion-assisted deposition.[10,28] The substrate consists of five layers of 40 atoms in a row and a total of 500 vapor atoms approach sequentially the surface of the growing film. While the ion-to-vapor flux ratio and the ion energy are varied the vapor arrival sequence is always the same. Figure 4(a) shows the microstructure obtained without ion bombardment (0.1-eV monoenergetic vapor atoms) and Figs. 4(b) and 4(c) with 50-eV Ar ion bombardment where the ion-to-vapor flux ratio is $j_I/j_V=0.04$ and 0.16, respectively. (Here, the Lennard-Jones potential $U_{\rm LJ}$ is used.) The reason for the formation of a columnar microstructure [Fig. 4(a)], even at 0° angle of vapor incidence, is due to

the attractive force between the atoms which curves the trajectories of vapor atoms towards adjacent atomic clusters. The sputtering yield found is about 0.35. In none of the examined cases were Ar ions entrapped in the film.

The packing densities, defined as the fraction of atoms occupying the first nine layers above the substrate, are shown in Fig. 5 for the two ion energies $E=10$ and 50 eV. The density increases with ion-to-vapor-flux ratio j_I/j_V. Because of the relatively small number of atoms involved in the simulation, limited by the otherwise unacceptable time of computation, the data exhibit considerable scattering but the trends are discernable. (An almost linear increase in packing density has been found experimentally for ion-assisted vapor deposited ZrO_2 and CeO_2 films.[10,28]) How the microstructure changes for a fixed ion-to-vapor flux ratio of $j_I/j_V=0.16$ with increasing ion kinetic energy E is displayed in Fig. 6. The sputtering yields are $y=0$ for $E=10$ eV and about 0.7 for $E=75$ eV. (The sputtering yields might be unrealistically high due to the above-mentioned restricted degrees of freedom in a 2D MD simulation.) The density is shown in Fig. 7 where the compound potential U results in a slightly larger packing density. The density increases rapidly at low ion energies because a weakly bonded porous structure is easier to reorder and densify than a more closely packed one. The interesting regime of ion kinetic energies larger than 100 eV could not be considered at present as the required larger relaxation time, which follows each ion-induced collision sequence, makes calculations very computer-time intensive.

To illustrate the improvement in homoepitaxial growth with increasing ratio j_I/j_V, Figs. 8(a)—8(c) show the

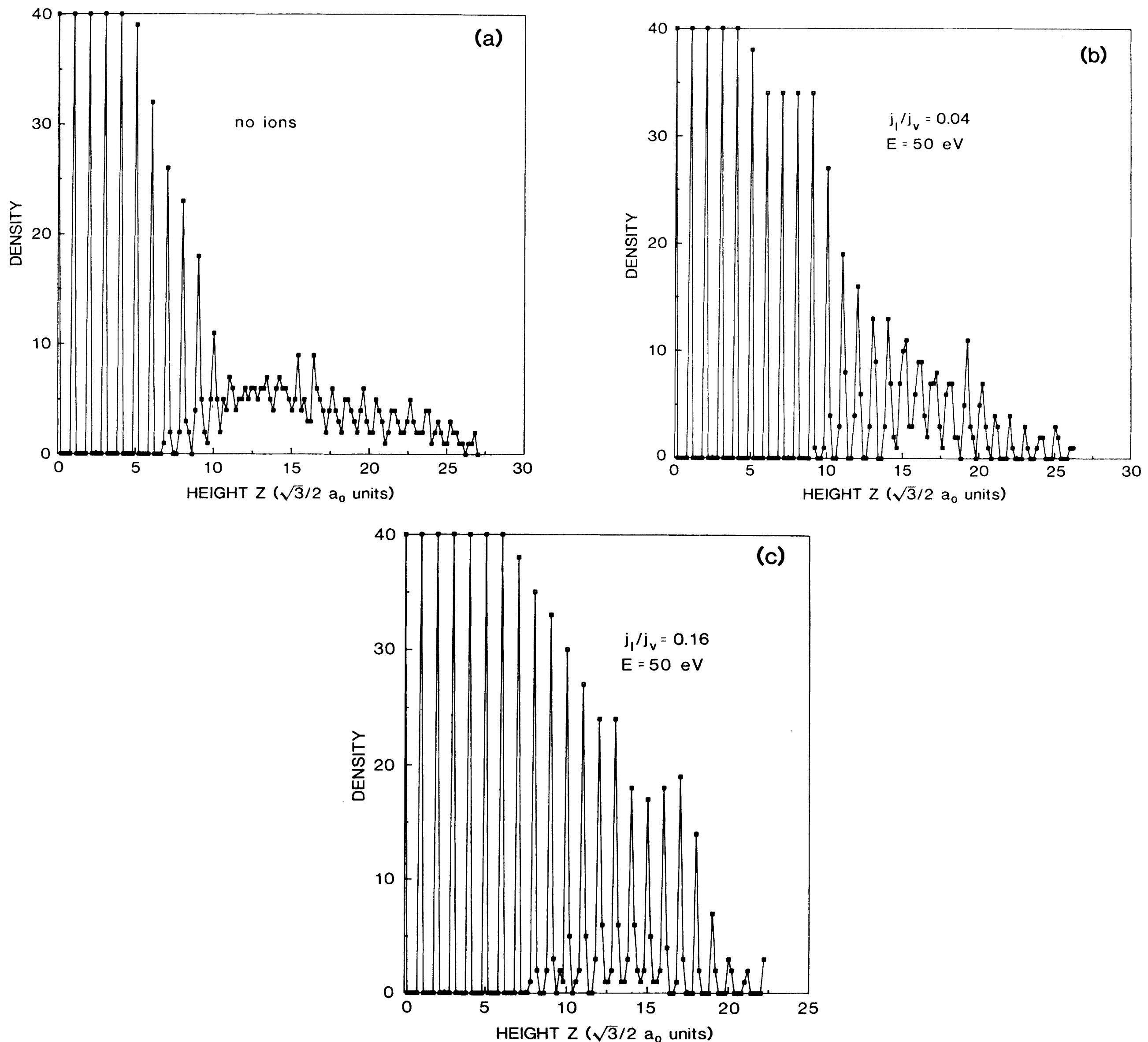

FIG. 8. (a)—(c) Atomic density vs height z at Ar ion kinetic energy of 50 eV for (a) no ions, (b) $j_I/j_V=0.04$, (c) $j_I/j_V=0.16$.

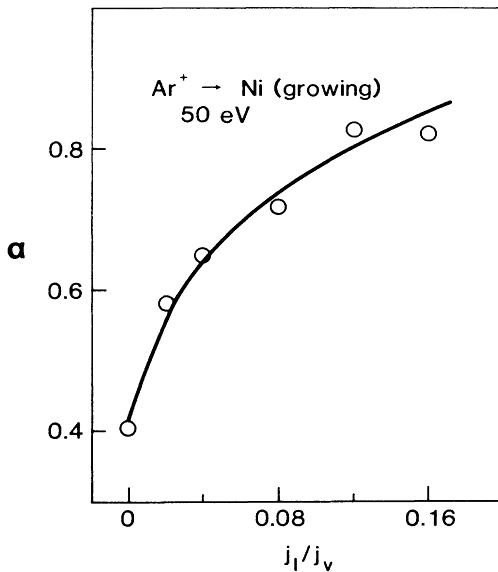

FIG. 9. Degree of homoepitaxy α in dependence of the ion-to-vapor flux ratio j_I/j_V for Ar^+ kinetic energy of $E=50$ eV. The atom-atom potential is U_{LJ}.

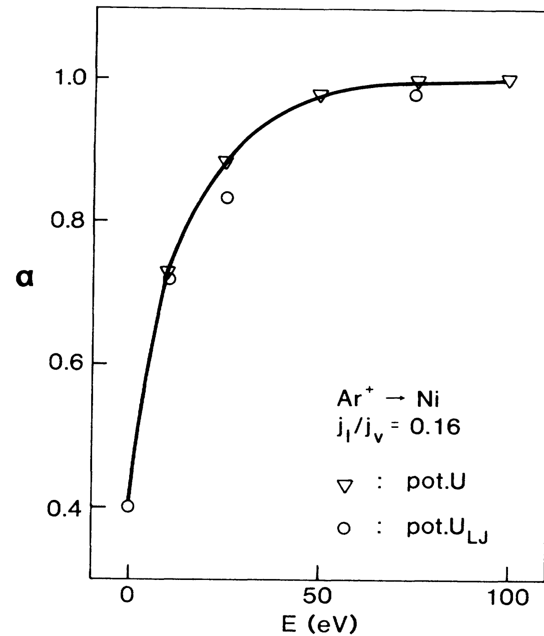

FIG. 10. The degree of homoepitaxy α vs ion kinetic energy E for a fixed ratio $j_I/j_V=0.16$. Results for potentials U and U_{LJ} are shown.

atomic density versus the height of the film corresponding to the microstructures of Figs. 4(a)—4(c). Here the atomic density is defined as the number of atoms found per height interval $\Delta z=(\sqrt{3}/10)a_0$. The substrate layers are included. Figure 8(a) indicates disorder in the deposited film, while Figs. 8(b) and 8(c) exhibit improved homoepitaxy. To illustrate the dependence of epitaxial growth on deposition parameters more quantitatively, we define the degree of homoepitaxial growth α as the portion of the condensed atoms located within narrow bands of width Δz around the ideal layers at positions $z=n(\sqrt{3}/2)a_0$, where $n=5,6,7,\ldots$. By this definition the value of $\alpha=0.2$ indicates no homoepitaxy while $\alpha=1$ corresponds to perfect epitaxy. Figure 9 shows how α depends on the ratio j_I/j_V for a fixed Ar ion energy of 50 eV. Plotting α versus the ion kinetic energy E for a fixed ratio $j_I/j_V=0.16$, as illustrated in Fig. 10, reveals a rather sudden increase in the low-energy region and perfect epitaxy is attained for an ion kinetic energy larger than about 50 eV. Again, there is a slight difference in the results for the two potentials used.

IV. CONCLUSION

A molecular-dynamics calculation is employed to study the atomic rearrangement processes occurring when porous thin films are bombarded by ions during growth. Although the model is only two-dimensional and therefore restricts deposition and relaxation processes, it is believed to reflect a number of essential features. The most important ion surface interaction processes which lead to microstructure modifications are (i) atoms accumulated to form a void structure are dislodged and forward sputtered by incoming ions causing the void region to remain open until filled by new depositing atoms; (ii) ion impacts induce surface diffusion as well as local heating such that recrystallization takes place during growth and the underlying crystal structure is adopted. In the 2D MD calculations up to 800 particles have been used to describe Ar^+-assisted Ni growth at zero substrate temperature. It has been shown that ion bombardment during growth enhances the adatom mobility, causing packing density and crystal order to increase with increasing ion-to-vapor flux ratio and ion energy. Ion-to-vapor flux ratios up to 0.16 and ion energies as high as 100 eV have been considered. The results are only slightly dependent on the two atom-atom potentials used. For all cases Ar was not entrapped in the film.

ACKNOWLEDGMENTS

The author would like to acknowledge P. J. Martin and A. F. Collings for stimulating discussions and express his thanks to the Division of Computing Research for their cooperation. The calculations were done on a CDC Cyber 205 computer.

[1]T. Takagi, Thin Solid Films **92**, 1 (1982).
[2]J. M. E. Harper, J. J. Cuomo, R. Gambino, and H. R. Kaufman, in *Ion Bombardment Modification of Surfaces,* edited by O. Auciello and R. Kelly (Elsevier, Amsterdam, 1984), p. 127.
[3]P. J. Martin, J. Mater. Sci. **21**, 1 (1986).
[4]M. Marinov, Thin Solid Films **46**, 267 (1977).
[5]J. E. Griffith, Y. Oiu, and T. A. Tombrello, Nucl. Instrum. Methods **198**, 607 (1982).
[6]D. Dobrev, Thin Solid Films **92**, 41 (1982).
[7]J. J. Cuomo, J. M. E. Harper, C. R. Guarnieri, D. S. Yee, L. J. Attanasio, J. Angilello, C. T. Wu, and R. H. Hammond, J. Vac. Sci. Technol. **20**, 349 (1982).
[8]K. Meyer, I. K. Schuller, and C. M. Falco, J. Appl. Phys. **52**, 5803 (1981).
[9]N. Savvides and B. Window, J. Vac. Sci. Technol. A **4**, 504 (1986).
[10]P. J. Martin, R. P. Netterfield, and W. G. Sainty, J. Appl. Phys. **55**, 235 (1984).
[11]K.-H. Müller, J. Vac. Sci. Technol. A **4**, 184 (1986).
[12]K.-H. Müller, J. Appl. Phys. **59**, 2803 (1986).
[13]K.-H. Müller, Appl. Phys. A **40**, 209 (1986).
[14]H. J. Leamy, G. H. Gilmer, and A. G. Dirks, in *Current Topics in Materials Sciences,* edited by E. Kaldis (North-Holland, Amsterdam, 1980), p. 309.
[15]D. Henderson, M. H. Brodsky, and P. Caudhari, Appl. Phys. Lett. **25**, 641 (1974).
[16]M. Schneider, A. Rahman, and I. K. Schuller, Phys. Rev. Lett. **55**, 604 (1985).
[17]D. E. Harrison, Jr., Radiation Effects **70**, 1 (1983).
[18]B. A. Movchan and A. V. Demchishin, Fiz. Met. Metalloved. **28**, 653 (1969).
[19]A. G. Dirks and H. J. Leamy, Thin Solid Films **47**, 219 (1977).
[20]S. Kim and D. J. Henderson, Thin Solid Films **47**, 155 (1977).
[21]K.-H. Müller, J. Appl. Phys. **58**, 2573 (1985).
[22]G. Moliere, Z. Naturforsch. A **2**, 133 (1947).
[23]O. B. Firsov, Zh. Eksp. Teor. Fiz. **33**, 696 (1957) [Sov. Phys.—JETP **6**, 534 (1958)].
[24]L. W. Johnson and R. D. Riess, *Numerical Analysis* (Addison-Wesley, Massachusetts, 1982), p. 237.
[25]D. E. Harrison, Jr., W. L. Gay, and H. M. Effran, J. Math. Phys. **10**, 1179 (1969).
[26]F. Sullivan, R. D. Mountain, and J. O'Connell, J. Comp. Phys. **61**, 138 (1985).
[27]D. M. Heyes, M. Barber, and J. H. R. Clarke, Surf. Sci. **105**, 225 (1981).
[28]R. P. Netterfield, W. G. Sainty, P. J. Martin, and S. H. Sie, Appl. Opt. **24**, 2267 (1985).